The Mechanism of the Porphyrin Spectral Shift on Inorganic Nanosheets: The Molecular Flattening Induced by the Strong Host–Guest Interaction due to the "Size-Matching Rule"

ARTICLE *in* THE JOURNAL OF PHYSICAL CHEMISTRY C · MARCH 2012

Impact Factor: 4.77 · DOI: 10.1021/jp300842f

6 AUTHORS, INCLUDING:

Shinsuke Takagi
Tokyo Metropolitan University
86 PUBLICATIONS **1,489** CITATIONS

SEE PROFILE

THE JOURNAL OF PHYSICAL CHEMISTRY C

Article

pubs.acs.org/JPCC

The Mechanism of the Porphyrin Spectral Shift on Inorganic Nanosheets: The Molecular Flattening Induced by the Strong Host–Guest Interaction due to the "Size-Matching Rule"

Yohei Ishida,[†,‡] Dai Masui,[†] Tetsuya Shimada,[†] Hiroshi Tachibana,[†] Haruo Inoue,[†] and Shinsuke Takagi*[,†,§]

[†]Department of Applied Chemistry, Graduate Course of Urban Environmental Sciences, Tokyo Metropolitan University, Minami-ohsawa 1-1, Hachiohji, Tokyo 192-0397 Japan

[‡]Japan Society for the Promotion of Science (DC1), Ichibancho, Chiyoda-ku, Tokyo 102-8471, Japan

[§]PRESTO (Precursory Research for Embryonic Science and Technology), Japan Science and Technology Agency, 4-1-8 Honcho Kawaguchi, Saitama, Japan

Supporting Information

ABSTRACT: The mechanism inducing the unique absorption spectral shifts of porphyrin molecules upon adsorption on the clay surface was experimentally confirmed to be the flattening of the meso substituent with respect to the plane of the porphyrin ring. We investigated the spectral shift systematically by using seven types of porphyrin derivatives, differing in their center metal, meso substituent, and number of cationic sites. The aggregation, which usually induces the spectral shift, is suppressed in our clay/porphyrin systems. The adsorption strengths of porphyrin molecules on the clay surface were estimated as the relative adsorption equilibrium constants K_{rel}. The seven types of porphyrins studied had different values of K_{rel}, which can be explained by the steric effect and the Coulomb interaction due to the differences in the molecular structure. The obtained K_{rel} values have interesting information of the photochemical property of the clay/porphyrin complexes. The absorption spectral shifts of the porphyrin Soret bands between those in the bulk solution and those on the clay surface are well related to K_{rel} values. Like this, by the systematic experiments using the series of porphyrin derivatives, it was directly confirmed that the flattening of the molecule is the dominant mechanism for the spectral shift on the surface of inorganic nanosheets.

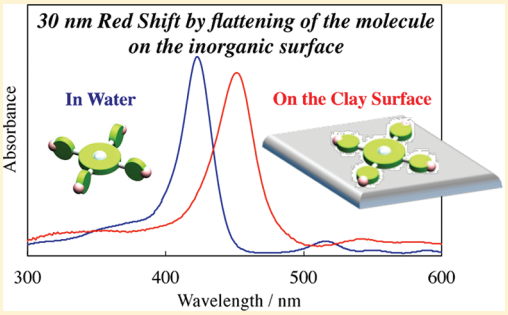

INTRODUCTION

We have been investigating inorganic/organic hybrids from a viewpoint of photochemistry.[1−8] In inorganic/organic systems, an interaction between the host materials and the guest molecules is crucially important to determine the various properties of the guest molecules. Over a number of years, there has been a large volume of literature concerning the interactions between organic molecules and inorganic materials.[9−40] With regard to the photochemical properties, the spectral shift of the absorption in functional dye complexes on the surface of inorganic nanosheets has been extensively studied. In the past, various mechanisms have been proposed for inducing the spectral shift of dyes on the surface of inorganic nanosheets as follows.[17−40] (i) "An effect of an aggregation of molecules".[17−23] This is the most usual mechanism for the spectral shift on the surface of inorganic nanosheets. Because organic molecules typically tend to be aggregated on the surface of inorganic nanosheets, the spectral shift is easily induced. (ii) "An effect of a solvent polarity".[24−26] This induces a few nanometers of spectral shift. (iii) "An effect of a protonation".[27−29] This was proposed for organic molecules that have pyridyl and/or pyrrole substituents, such as for the free-base pyrrole in porphyrin derivatives. (iv) "An effect of an external electric field".[30,31] Yariv et al. proposed the mechanism due to the π-electron interactions between the adsorbed dyes and the oxygen plane of the alumino-silicate. (v) "An effect of a conformation change upon adsorption on the surface of inorganic nanosheets".[4−7,25,26,29,32−40] This mechanism is typically due to the flatness of the surface of inorganic nanosheets.

Because the aggregation of molecules cannot be suppressed in usual inorganic/organic systems, investigations for the spectral shift tend to be complicated. Thus, the detailed systematic investigation has not been completed. In constant, we have reported an interesting clay/porphyrin complex whose cationic porphyrin molecules adsorb on an anionic clay surface without aggregation even under high dye loadings.[4−7] Because the aggregation of porphyrin molecules is completely suppressed by the "size-matching rule" (as described later), the mechanism for inducing the spectral shift can be simply

Received: January 26, 2012
Revised: March 16, 2012
Published: March 16, 2012

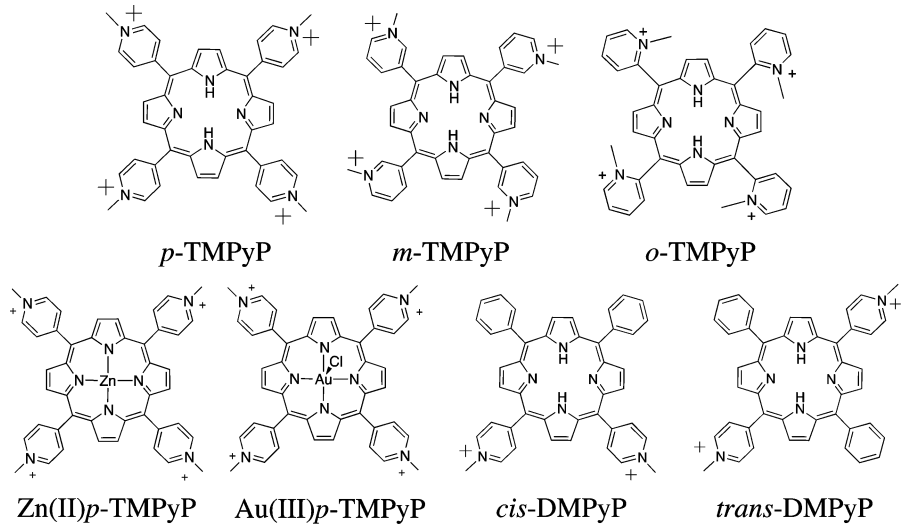

Figure 1. Structures of porphyrins.

discussed. By using a series of porphyrin derivatives, differing in their center metal, meso substituent, and number of cationic sites, the mechanisms of the spectral shift upon adsorption on the clay surface can be systematically investigated.

The details of our clay/porphyrin complexes are as follows. Saponite,[41−50] which is one of the typical clay minerals, is used as inorganic nanosheets. Saponite[41−50] is a group of materials that are characterized by (1) nanostructured flat sheets, (2) negatively charged surfaces, (3) exfoliation or stack ability of individual nanosheets depending on the surrounding conditions, and (4) optical transparency in the visible region in the exfoliated state, when the particle size is small (ca. <200 nm). The formation of a unique nonaggregated porphyrin assembly on the clay surface was elucidated by "size-matching" of the distances between the charged sites in the porphyrin molecule and those between the anionic sites on the clay surface. We termed this effect the "size-matching rule".[4−7] An aggregation is defined as an interaction between the transition dipole moments of dyes under the ground state. In the present paper, the adsorption strength of a series of porphyrin derivatives is estimated as the relative adsorption equilibrium constants K_{rel}. The relationships between the K_{rel} values and the maximum adsorption amount and the absorption spectral shift are discussed.

EXPERIMENTAL SECTION

Materials. The saponite clay used in this experiment was synthesized by hydrothermal synthesis according to a previous paper.[7] Na_2SiO_3 solution (15.45 g) was diluted by the addition of 80 mL of deionized water, and then 5 mL of nitric acid solution was added to the diluted Na_2SiO_3 solution (Solution A). A 12.44 g portion of $MgCl_2$ $6H_2O$ and 1.97 g of $AlCl_3$ $6H_2O$ were dissolved in 20 mL of deionized water (Solution B). Solutions A and B were combined, and the obtained solution was added to 52 mL of ammonia solution under continuous stirring within approximately 3 min. The formed precipitate was filtered with a glass filter (type 25G3) and washed with deionized water repeatedly. A 5 mL portion of an aqueous solution of NaOH (1.55 M) was added to the collected residue. The obtained slurry was kept under 573 K and 8.5 MPa in the autoclave for about 6 h. The saponite component was collected from the reaction mixture by 3 days hydraulic elutriation and a centrifugal separation of the supernatant (18 000 rpm, 5 h). The synthetic saponite was analyzed with XRD, XRF,[27]Al-NMR, FT-IR, and TG/DTA. The cation-exchange capacity (CEC) was 1.00 meq g^{-1}, and the average intercharge distance on the clay surface was calculated to be 1.19 nm on the basis of a hexagonal array. Tetrakis(1-methylpyridinium-4-yl) porphyrin (*p*-TMPyP), tetrakis(1-methylpyridinium-3-yl) porphyrin (*m*-TMPyP), tetrakis(1-methylpyridinium-2-yl) porphyrin (*o*-TMPyP), tetrakis(1-methylpyridinium-4-yl) porphyrinatozinc (Zn(II)*p*-TMPyP), tetrakis(1-methylpyridinium-4-yl) porphyrinato(chloride)gold-(III) (Au(III)*p*-TMPyP), *cis*-bis(1-methylpyridinium-4-yl) diphenylporphyrin (*cis*-DMPyP), *trans*-bis(1-methylpyridinium-4-yl) diphenylporphyrin (*trans*-DMPyP) were purchased from Frontier Scientific (Figure 1). The counterions were exchanged for chloride by use of an ion-exchange column (Organo Amberlite IRA400JCL). The purity of the porphyrins was checked by ^1H NMR. Water was deionized with an ORGANO BB-5A system (PF filter ×2 + G-10 column).

Analysis. Absorption spectra were measured with a Shimadzu UV-3150 spectrophotometer. In the measurements, a quartz cell was used for the aqueous clay/porphyrin solutions. TG/DTA measurement was carried out with a Shimadzu DTG-60H to determine the water content of the porphyrins and clay.

Preparation Methods for the Clay/Porphyrin Complexes. *Porphyrin/Clay Complexes for Determining the Maximum Adsorption Amount on the Clay Surface.* An aqueous porphyrin solution was mixed with an aqueous clay solution under vigorous stirring. The dye loadings were changed by changing the concentration of porphyrin. The concentration of clay was always kept constant at 8.0 mg L^{-1}. To express the dye loadings on the clay surface (% vs CEC of the clay), a porphyrin concentration ×4 was adopted, although *cis*- and *trans*-DMPyP have only two cationic sites. This expression excludes the confusion for understanding the adsorption density (molecule nm^{-2}) for each porphyrin. Under these conditions, the clay sheets exist as individually exfoliated sheets and the obtained solution was substantially transparent.

Estimation of the Relative Adsorption Equilibrium Constant. An aqueous solution of *p*-TMPyP was mixed with an aqueous clay solution under vigorous stirring ([clay] = 2.0

dx.doi.org/10.1021/jp300842f | J. Phys. Chem. C 2012, 116, 7879−7885

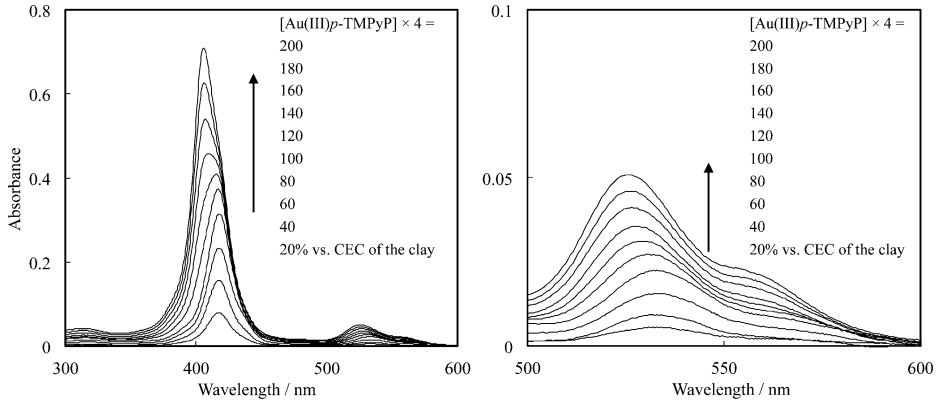

Figure 2. Absorption spectra of Au(III)*p*-TMPyP/clay complexes at various dye loadings up to 200% vs CEC in aqueous solution. Left: all wavelength regions. Right: Q-band absorption regions. The concentration of clay was 8.0 mg L^{-1}.

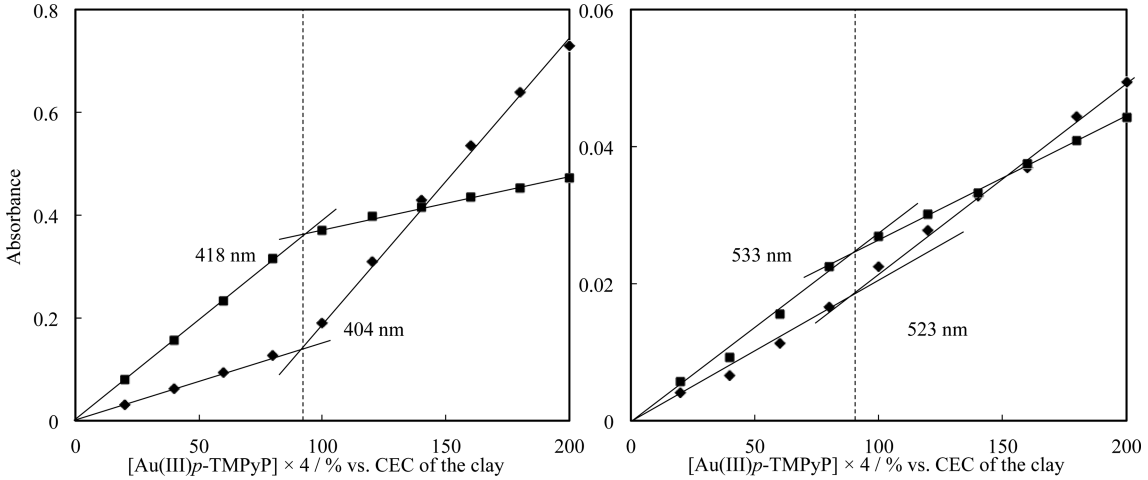

Figure 3. Absorbance−concentration plots for Au(III)*p*-TMPyP/clay complexes (left: Soret bands at 404 nm (◆) and 418 nm (■); right: Q-bands at 523 nm (◆) and 533 nm (■)) in aqueous solution. The dye loadings were changed from 20% to 200% vs CEC of the clay. The concentration of clay was 8.0 mg L^{-1}.

mg L^{-1}, 100% vs CEC). The obtained solution was then mixed with an aqueous solution of another porphyrin (50−200% vs CEC). The absorption spectrum reached to the equilibrium after a few minutes. Because the two types coadsorbed porphyrins exhibit no aggregation on the clay surface, the adsorbed amount of each porphyrin on the clay surface can be determined by the observed spectrum. The relative adsorption equilibrium constant of porphyrin molecules was calculated by the adsorbed and nonadsorbed amounts determined by the absorption spectra, according to eq 1, as described in the Results and Discussion section. In the case where *o*-TMPyP was used as additional porphyrin, the concentration of clay was changed to be 0.1 mg L^{-1} and the dye loadings were set at 50−20 000% because the adsorption strength of *o*-TMPyP was rather small.

■ RESULTS AND DISCUSSION

Absorption Spectra of Cationic Porphyrins on the Clay Surface. Absorption spectra of seven types of cationic porphyrins on the clay surface were observed. As we have reported, in the cases of *p*-TMPyP, Zn(II)*p*-TMPyP, *cis*-DMPyP, and *trans*-DMPyP, the adsorbed porphyrins exist as a single molecular unit at every loading level (0−100% vs CEC of the clay).[4−6] In the cases of *m*-TMPyP and *o*-TMPyP, the adsorbed porphyrins exist as a single molecule for 0−85% and 0−75% vs CEC of the clay, respectively.[4−6]

The absorption spectra of Au(III)*p*-TMPyP on the clay surface were observed at various dye loadings, as shown in Figure 2. Above 100% vs CEC adsorption, the observed spectra were composed of two components for Au(III)*p*-TMPyP. The long-wavelength absorption at 418 nm (533 nm for Q-band absorption) was the component of the adsorbed porphyrin on the clay surface, and short-wavelength absorption at 404 nm (523 nm for Q-band absorption) was the component of the nonadsorbed porphyrin in a bulk solution. The λ_{max} shift of the porphyrin upon adsorption on the clay surface has been proposed to be mainly dependent on the flattening of the meso substituents with respect to the porphyrin rings.[4−7,25,26,36−40] The absorbance concentration plot for Au(III)*p*-TMPyP/clay complexes are shown in Figure 3. As shown in Figure 3, the linearity of the plot was observed below 92% vs CEC of the clay. Thus, it turns out that the Au(III)*p*-TMPyP exists as a single molecule for 0−92% vs CEC in this condition. The maximum adsorption amounts of examined porphyrins are summarized in Table 1.

Estimation of the Adsorption Strength of Seven Types of Porphyrins on the Clay Surface. Following the experimental procedure in the Experimental Section, the adsorption strengths of seven types of porphyrins on the clay

dx.doi.org/10.1021/jp300842f | J. Phys. Chem. C 2012, 116, 7879−7885

Table 1. Maximum Adsorption Amount of Porphyrin Molecules on the Clay Surface

	maximum adsorption amount vs CEC of the clay
p-TMPyP	100%[a]
trans-DMPyP	100%[a]
cis-DMPyP	100%[a]
Zn(II)*p*-TMPyP	100%[b]
Au(III)*p*-TMPyP	92%
m-TMPyP	85%[a]
o-TMPyP	75%[a]

[a]Values refer to ref 6. [b]The value refers to ref 5.

surface were estimated as the relative adsorption equilibrium constants K_{rel} according to eq 1

$$P/\text{clay} + A \rightleftarrows A/\text{clay} + P \quad (1)$$

where P/clay and A/clay are the adsorbed amount of *p*-TMPyP and the additional porphyrin on the clay surface, respectively. P and A are the amount of *p*-TMPyP and the additional porphyrin in a bulk solution, respectively. The observed absorption spectra corresponded perfectly to the sum of individual absorption spectra of *p*-TMPyP and the additional porphyrin in the bulk solution and on the clay surface. An aggregation of porphyrin molecules was suppressed even when two porphyrins coadsorb on the clay surface; thus, the absorption spectrum of the mixture sample corresponded well to the calculated one for all absorption regions (400−700 nm). In the case of *trans*-DMPyP, the Soret-band absorption is rather the same as that of *p*-TMPyP within a few nanometers. However, due to the differences in Q-band absorption regions, we can determine the adsorbed and nonadsorbed amounts of each porphyrin (Figure S1 in the Supporting Information).

From eq 1, K_{rel} is expressed to eq 2

$$K_{rel} = \frac{[P][A/\text{clay}]}{[P/\text{clay}][A]} \quad (2)$$

Equation 2 can be rewritten to eq 3

$$\frac{[P/\text{clay}]}{[P]} = \frac{1}{K_{rel}}\frac{[A/\text{clay}]}{[A]} \quad (3)$$

According to eq 3, the observed values of $[P/\text{clay}]/[P]$ are plotted vs $[A/\text{clay}]/[A]$, as shown in Figure 4.

As a result, the plots can be fitted as straight lines with different slopes. From the slopes, the relative adsorption equilibrium constant K_{rel} was obtained, as summarized in Table 2.

The differences in K_{rel} can be qualitatively explained by porphyrin structures as follows. In the cases of *p*-TMPyP, Zn(II)*p*-TMPyP, and Au(III)*p*-TMPyP, the differences of K_{rel} can be explained by the steric effect of center metals. From the viewpoint of the size of metal, the van der Waals' radii of Zn(II) and Au(III) are 0.74 and 0.91 Å, respectively.[51] The axial ligand Cl of Au(III)*p*-TMPyP also acts as a factor of steric hindrance. Thus, these differences are reasonable.

In the cases of *p*-TMPyP, *m*-TMPyP, and *o*-TMPyP, these differences of K_{rel} can be rationalized by the Coulomb interaction between cationic sites of the porphyrin and the anionic sites of the clay surface. Because the Coulomb attraction energy is inversely proportional to the distance between charged sites of porphyrin and the clay surface,[52] the size-matching degree of each porphyrin to the clay surface

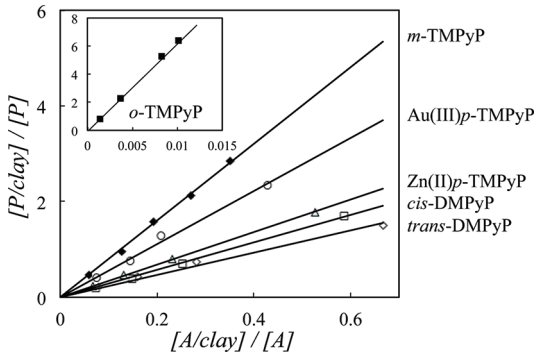

Figure 4. Observed values of $[P/\text{clay}]/[P]$ are plotted vs $[A/\text{clay}]/[A]$. The values of $[P/\text{clay}]/[P]$ and $[A/\text{clay}]/[A]$ were determined by the absorption spectra of two types of porphyrin/clay complexes in the aqueous solution. The loading level of *p*-TMPyP was set at 100% vs CEC of the clay. The loading levels of additional porphyrins were set at 50−200% vs CEC of the clay. The concentration of clay was 2.0 mg L^{-1}. Inset: in the case of *o*-TMPyP. The concentration of clay was 0.1 mg L^{-1}. The dye loadings were set at 50−20 000%, because the K_{rel} of *o*-TMPyP was rather small.

Table 2. Relative Adsorption Equilibrium Constant K_{rel}[a]

	K_{rel}
p-$TMPyP^{4+}$	1
trans-$DMPyP^{2+}$	0.43
cis-$DMPyP^{2+}$	0.35
Zn(II)*p*-$TMPyP^{4+}$	0.3
Au(III)*p*-$TMPyP^{4+}$	0.18
m-$TMPyP^{4+}$	0.12
o-$TMPyP^{4+}$	1.6×10^{-3}

[a]*p*-TMPyP is used as a standard of K_{rel}.

crucially affects the adsorption strengths. In the present system, the average interanionic charge distance on the clay surface is 1.19 nm on the basis of a hexagonal array. The intracationic distances of *p*-TMPyP, *m*-TMPyP, and *o*-TMPyP are calculated to be 1.05, 0.99, and 0.88 nm from the AM1 method,[4−6] respectively; thus, the differences of K_{rel} are rationalized by the intracationic charge distance of porphyrin molecules.

In addition, amazingly, the adsorption strengths of *trans*-DMPyP and *cis*-DMPyP were larger than others without *p*-TMPyP, despite the fact that they have only two cationic sites. This cannot be explained by the electrostatic interaction. We assumed that this was due to the smaller bulkiness of the meso-substituted phenyl groups. The solubility of *trans*-DMPyP and *cis*-DMPyP in aqueous solution should also play an important role in the large K_{rel}, because the solubility of dicationic porphyrins in water is smaller than that of tetracationic porphyrins.

The maximum adsorption amounts of examined porphyrins (Table 1) are plotted vs obtained K_{rel} (Table 2) in Figure 5. As shown in Figure 5, a good correlation was observed between the maximum adsorption amount and K_{rel}. Because the saturated adsorption amount of organic molecules is typically governed by the adsorption strength between guest molecules and host materials, these correlations are reasonable. Below the steady value of K_{rel} (about 0.2−0.3, judging from Figure 5), the repulsion force between cationic sites in porphyrin molecules induces the nonmaximum adsorption on the clay surface.

Relationship between K_{rel} and the Absorption Spectral Shift of Porphyrin Molecules on the Clay

dx.doi.org/10.1021/jp300842f | J. Phys. Chem. C 2012, 116, 7879−7885

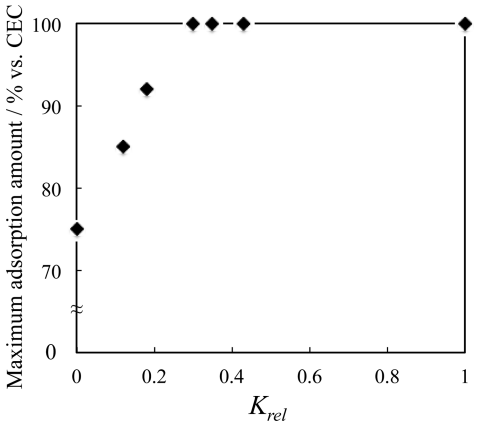

Figure 5. Relationship between the maximum adsorption amounts of porphyrin molecules on the clay surface (% vs CEC) and K_{rel}.

Surface. The correlation between K_{rel} and the absorption spectral shift of the porphyrin molecule on the clay surface was studied. Porphyrin has two important absorption regions, that is, Q-bands and Soret bands. Since the spectral shifts in the Soret band were clearer than those in Q-bands, in this study, the degrees of spectral shifts were defined as the changes of the λ_{max} of the Soret band between those in a bulk solution and those adsorbed on the exfoliated clay surface. The values of spectral shifts in porphyrin Q-bands are described in the Supporting Information. The values of red shifts $\Delta\lambda_{max}$ and λ_{max} of the porphyrins in water and λ_{max} of porphyrin on the clay surface are summarized in Table 3. For clarity, $\Delta\lambda_{max}$ were plotted versus K_{rel} in Figure 6.

Table 3. Values of Red Shifts $\Delta\lambda_{max}$ (in nm and in cm^{-1}), λ_{max} in Water, and λ_{max} on the Clay Surface (in nm)

	$\Delta\lambda_{max}$/nm (cm^{-1})	λ_{max} in water/nm	λ_{max} on the clay surface/nm
cis-DMPyP	36 (1.89×10^3)	419	455
p-TMPyP	30 (1.58×10^3)	421	451
Zn(II)*p*-TMPyP	27 (1.34×10^3)	435	462
trans-DMPyP	26 (1.39×10^3)	419	445
Au(III)*p*-TMPyP	14 (8.29×10^2)	404	418
m-TMPyP	12 (6.74×10^2)	416	428
o-TMPyP	6 (3.45×10^2)	414	420

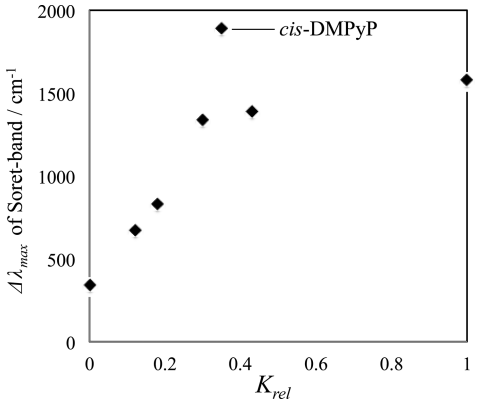

Figure 6. Relationship between $\Delta\lambda_{max}$ of the Soret band (cm^{-1}) and K_{rel}.

As a result, a good correlation between $\Delta\lambda_{max}$ and K_{rel} was observed. It was found that the adsorption strength of porphyrin molecules on the clay surface plays an important role for inducing the spectral shift. The good correlation was also observed for the spectral shift in Q-bands. The various mechanisms for the absorption spectral shift have been proposed.[17−40] Among them, the mechanism (i) "an aggregation" can be excluded by the "size-matching rule". The mechanism (ii) "a solvent polarity" also can be negligible because it induces only small spectral shifts (2−3 nm for *p*-TMPyP).[25] The mechanism (iii) "a protonation of the free-base pyrrole nitrogen" can be excluded because the four Q-band absorptions of free-base porphyrins were observed on the clay surface. Judging from the reduction potentials of some of the porphyrins (−1.02, −1.15, −1.26, and −0.85 V vs Ag/AgCl for *p*-TMPyP, *m*-TMPyP, *cis*-DMPyP, and Zn(II)*p*-TMPyP, respectively),[53−55] the mechanism (iv)[30,31] is not the dominant one, because there is no correlation between the $\Delta\lambda_{max}$ and the reduction potentials of porphyrins. In this π interaction, occupied nonbonding sp^2 orbitals of the basic oxygens from the O plane overlap the highest unoccupied antibonding π orbitals of the guest cations.[30] The $\pi \rightarrow \pi^*$ transition of the adsorbed guest molecule is associated with a higher energy gap due to the repulsion between electron pairs that were donated by the oxygens and the π electrons of the guest cation. Thus, the energy level of the unoccupied antibonding orbitals is raised and the $\pi \rightarrow \pi^*$ transition shifts to a lower wavelength.[30]

Thus, the major mechanisms for inducing the spectral shift can be focused on the mechanism (v), "an effect of a conformation change upon adsorption on the surface of inorganic nanosheets". In the case of porphyrin molecules, the mechanism (v) is classified into two mechanisms, that is, (v-i) "an effect of a ruffled structure of the porphyrin ring"[29,32−35] and (v-ii) "an effect of a flattening of the meso substituent with respect to the plane of the porphyrin ring".[4−7,25,26,36−40] Judging from the good correlation between the spectral shifts and the adsorption equilibrium constants in Figure 6, the effect of the center metal does not contribute for the mechanism (v-i) dominantly. The spectral shift due to the mechanism (v-ii) is dependent on a couple of reasons.[56−58] First, the molecular flattening will extend the π-conjugation of the porphyrin molecule. Second, the resonance electron-withdrawing effect of meso-substituted methylpyridinium groups will be enhanced, suggesting that both HOMO and LUMO will be stabilized, especially for LUMO.[56−58] Thus, when the meso substituents rotate toward the coplanar conformation with respect to the porphyrin ring (i.e., flattening), the absorption spectrum will shift to the longer wavelength, which corresponds to the decrease of the HOMO−LUMO gap. By the DFT calculation, the effect of the molecular flattening on the spectral behavior was qualitatively reproduced. When the dihedral angle from the vertical was changed from 80° to 50°, the calculated absorption spectrum exhibited about a 30 nm red shift (Figure S3 in the Supporting Information). Judging from the result of Figure 6, it is apparent that the mechanism (v-ii) is the dominant one in the present system.

cis-DMPyP is not correlated well with Figure 6. We assumed that this mismatching is probably due to the mechanism (v-i), because *cis*-DMPyP has little symmetric structure compared to the others.[32−35] According to the literature, the ruffled porphyrin ring induces a red shift.[32−35] Like this, by the systematic experiments using the series of porphyrin derivatives, it was directly confirmed that the flattening of the

dx.doi.org/10.1021/jp300842f | J. Phys. Chem. C 2012, 116, 7879−7885

molecule is the dominant mechanism for the spectral shift on the surface of inorganic nanosheets.

CONCLUSION

The mechanism inducing the unique absorption spectral shifts of porphyrin molecules upon adsorption on the clay surface was experimentally confirmed to be the flattening of the meso substituent with respect to the plane of the porphyrin ring. We systematically investigated the spectral shift by using seven types of porphyrin derivatives, differing in their center metal, meso substituent, and number of cationic sites. In our clay/porphyrin system, the aggregation of porphyrin molecules is completely suppressed by the previously reported "size-matching rule". Because the aggregation, which is the typical major mechanism for the spectral shift, can be ruled out, we can simply investigate the spectral shift on the surface of inorganic nanosheets. The adsorption strengths of porphyrin molecules on the clay surface, which is related to the porphyrin structural change, were estimated as the relative adsorption equilibrium constants K_{rel}. The seven types of porphyrins studied had different values of K_{rel}, which can be explained by the steric effect and the Coulomb interaction due to the difference in the molecular structure. Among the examined porphyrins, tetrakis-(1-methylpyridinium-4-yl) porphyrin (*p*-TMPyP) adsorbed strongest on the surface of inorganic nanosheets. The obtained K_{rel} values have interesting information of the photochemical and physicochemical properties of the clay/porphyrin complexes. With regard to the physicochemical properties, the maximum adsorption amount of porphyrin molecules was rationalized by K_{rel} values. Moreover, the absorption spectral shifts of the porphyrin Soret bands between those in the bulk solution and those on the clay surface are well related to K_{rel} values, where photochemical properties are concerned. Like this, it was found that the host (clay)−guest (molecule) interaction governs the adsorption and spectral behavior of porphyrin molecules on the surface of inorganic nanosheets. The major mechanism for the spectral shift of porphyrin molecules on the surface of inorganic nanosheets was experimentally confirmed to be the flattening of the molecule.

ASSOCIATED CONTENT

Supporting Information

The experimental details for the determination of the adsorption equilibrium constants, the spectral shifts in Q-band absorption, and the DFT calculation for the spectral shift behavior depending on the dihedral angles. This material is available free of charge via the Internet at http://pubs.acs.org.

AUTHOR INFORMATION

Corresponding Author

*E-mail: takagi-shinsuke@tmu.ac.jp. Tel: +81 42 677 2839. Fax: +81 42 677 2838.

Notes

The authors declare no competing financial interest.

ACKNOWLEDGMENTS

This work has been partly supported by a Grant-in-Aid for Precursory Research for Embryonic Science and Technology (PRESTO) from the Japan Science and Technology Agency (JST), and JSPS Research Fellow DC1 from the Japan Society for the Promotion of Science.

REFERENCES

(1) Takagi, S.; Tryk, D. A.; Inoue, H. *J. Phys. Chem. B* **2002**, *106*, 5455−5460.
(2) Takagi, S.; Eguchi, M.; Tryk, D. A.; Inoue, H. *Langmuir* **2006**, *22*, 1406−1408.
(3) Ishida, Y.; Shimada, T.; Masui, D.; Tachibana, H.; Inoue, H.; Takagi, S. *J. Am. Chem. Soc.* **2011**, *133*, 14280−14286.
(4) Takagi, S.; Shimada, T.; Yui, T.; Inoue, H. *Chem. Lett.* **2001**, *30*, 128−129.
(5) Takagi, S.; Shimada, T.; Eguchi, M.; Yui, T.; Yoshida, H.; Tryk, D. A.; Inoue, H. *Langmuir* **2002**, *18*, 2265−2272.
(6) Eguchi, M.; Takagi, S.; Tachibana, H.; Inoue, H. *J. Phys. Chem. Solids* **2004**, *65*, 403−407.
(7) Egawa, T.; Watanabe, H.; Fujimura, T.; Ishida, Y.; Yamato, M.; Masui, D.; Shimada, T.; Tachibana, H.; Inoue, H.; Takagi, S. *Langmuir* **2011**, *27*, 10722−10729.
(8) Takagi, S.; Eguchi, M.; Yui, T.; Inoue, H. *Clay Sci.* **2006**, *12* (Suppl. 2), 82−87.
(9) Yui, T.; Kobayashi, Y.; Yamada, Y.; Yano, K.; Fukushima, Y.; Torimoto, T.; Takagi, K. *ACS Appl. Mater. Interfaces* **2011**, *3*, 931−935.
(10) Thomas, K. J.; Sunoj, R. B.; Chandrasekhar, J.; Ramamurthy, V. *Langmuir* **2000**, *16*, 4912−4921.
(11) Inagaki, S.; Ohtani, O.; Goto, Y.; Okamoto, K.; Ikai, M.; Yamanaka, K.; Tani, T.; Okada, T. *Angew. Chem., Int. Ed.* **2009**, *48*, 4042−4046.
(12) Casey, J. P.; Bachilo, S. M.; Weisman, R. B. *J. Mater. Chem.* **2008**, *18*, 1510−1516.
(13) Schanze, K.; Silverman, E. E.; Zhao, X. *J. Phys. Chem. B* **2005**, *109*, 18451−18459.
(14) Kaschak, D. M.; Lean, J. T.; Waraksa, C. C.; Saupe, G. B.; Usami, H.; Mallouk, T. E. *J. Am. Chem. Soc.* **1999**, *121*, 3435−3445.
(15) Fujii, K.; Iyi, N.; Hashizume, H.; Shimomura, S.; Ando, T. *Chem. Mater.* **2009**, *21*, 1179−1181.
(16) Pushpito, G. K.; Bard, A. *J. Phys. Chem.* **1984**, *88*, 5519−5526.
(17) Grauer, Z.; Avnir, D.; Yariv, S. *Can. J. Chem.* **1984**, *62*, 1889−1894.
(18) Czimerova, A.; Jankovic, L.; Bujdak, J. *J. Colloid Interface Sci.* **2004**, *274*, 126−132.
(19) Itho, T.; Shichi, T.; Yui, T.; Takahashi, H.; Takagi, K. *Chem. Lett.* **2004**, *33*, 1268−1269.
(20) Worsfold, O.; Dooling, C. M.; Richardson, T. H.; Vysotsky, M. O.; Tregonning, R.; Hunter, C. A.; Malins, C. *J. Mater. Chem.* **2001**, *11*, 399−403.
(21) Miyamoto, N.; Kawai, R.; Kuroda, K.; Ogawa, M. *Appl. Clay Sci.* **2000**, *16*, 161−170.
(22) Bujdak, J.; Iyi, N. *Clays Clay Miner.* **2002**, *50*, 446−454.
(23) Iyi, N.; Sasai, R.; Fujita, T.; Deguchi, T.; Sota, T.; Lopez Arbeloa, F.; Kitamura, K. *Appl. Clay Sci.* **2002**, *22*, 125−136.
(24) Yariv, S.; Ghosh, D. K.; Hepler, L. G. *J. Chem. Soc., Faraday Trans.* **1991**, *87*, 1201−1207.
(25) Chernia, Z.; Gill, D. *Langmuir* **1999**, *15*, 1625−1633.
(26) Kuykendall, V. G.; Thomas, J. K. *Langmuir* **1990**, *6*, 1350−1356.
(27) Kosiur, D. R. *Clays Clay Miner.* **1977**, *25*, 365−371.
(28) Cady, S. S.; Pinnavaia, T. J. *Inorg. Chem.* **1978**, *17*, 1501−1507.
(29) Dias, P. M.; Faria, D. L. A.; Constantino, V. R. L. *Clays Clay Miner.* **2005**, *53*, 361−371.
(30) Shweky, D. G.; Yariv, S. *J. Colloid Interface Sci.* **1997**, *188*, 168−175.
(31) Dobrogowska, C.; Hepler, L. G.; Ghosh, D. K.; Yariv, S. *J. Therm. Anal.* **1991**, *37*, 1347−1356.
(32) Wertsching, A. K.; Koch, A. S.; DiMagno, S. G. *J. Am. Chem. Soc.* **2001**, *123*, 3932−3937.
(33) Ryeng, H.; Ghosh, A. *J. Am. Chem. Soc.* **2002**, *124*, 8099−8103.
(34) Starukhin, A.; Shulga, A.; Waluk, J. *Chem. Phys. Lett.* **1997**, *272*, 405−411.
(35) Parusel, A. B. J.; Wondimagegn, T.; Ghosh, A. *J. Am. Chem. Soc.* **2000**, *122*, 6371−6374.

(36) Takagi, S.; Inoue, H. In *Multimetallic and Macromolecular Inorganic Photochemistry*; Ramamurthy, V., Schanze, K. S., Eds.; Marcel Dekker: New York, 1999; Vol. *6*, p 214.
(37) Xu, Y.; Bai, H.; Hong, W.; Li, C.; Shi, G. *J. Am. Chem. Soc.* **2009**, *131*, 13490−13497.
(38) Ou, Z.; Yao, H.; Kimura, K. *J. Photochem. Photobiol., A* **2007**, *189*, 7−14.
(39) Ou, Z.; Yao, H.; Kimura, K. *Chem. Lett.* **2006**, *35*, 782−783.
(40) Ceklovsky, A.; Czimerova, A.; Lang, K.; Bujdak, J. *Pure Appl. Chem.* **2009**, *81*, 1385−1396.
(41) Kuroda, T.; Fujii, K.; Sakoda, K. *J. Phys. Chem. C* **2010**, *114*, 983−989.
(42) Ogawa, M.; Kuroda, K. *Chem. Rev.* **1995**, *95*, 399−438.
(43) Lopez Arbeloa, F.; Martinez, V.; Arbeloa, T.; Lopez Arbeloa, I. *J. Photochem. Photobiol., C* **2007**, *8*, 85−108.
(44) Ras, R.; Umemura, Y.; Johnston, C.; Yamagishi, A.; Schoonheydt, R. *Phys. Chem. Chem. Phys.* **2007**, *9*, 918−932.
(45) Sato, H.; Hiroe, Y.; Tamura, K.; Yamagishi, A. *J. Phys. Chem. B* **2005**, *109*, 18935−18941.
(46) Letaief, S.; Detellier, C. *Langmuir* **2009**, *25*, 10975−10979.
(47) Takagi, K.; Shichi, T. *J. Photochem. Photobiol., C* **2000**, *1*, 113−130.
(48) Takagi, S.; Eguchi, M.; Tryk, D. A.; Inoue, H. *J. Photochem. Photobiol., C* **2006**, *7*, 104−126.
(49) Thomas, J. K. *Chem. Rev.* **1993**, *93*, 301−320.
(50) Bujdak, J. *Appl. Clay Sci.* **2006**, *34*, 58−73.
(51) Dean, J. A.; Lange, N. A. *Lange's Handbook of Chemistry*, 13th ed.; McGraw-Hill Inc.: New York, 1985; Section 3, pp 121−126.
(52) Isaacs, N. S. *Physical Organic Chemistry*; Longman Scientific & Technical: New York, 1987; pp 46−47.
(53) Willianms, R. F. X.; Hambright, P. *Bioinorg. Chem.* **1978**, *9*, 537−544.
(54) Kadish, K. M.; Araullo, C.; Maiya, G. B.; Sazou, D.; Barbe, J. M.; Guilard, R. *Inorg. Chem.* **1989**, *28*, 2528−2533.
(55) Shamim, A.; Hambright, P.; Willianms, F. X. *Inorg. Nucl. Chem. Lett.* **1979**, *15*, 243−246.
(56) Barbee, J.; Kuznetsov, E. A. *Comput. Theor. Chem.* **2012**, *981*, 73−85.
(57) Ma, R.; Gui, P.; Cui, H.; Zhang, X.; Nazeeruddin, K. M.; Gratzel, M. *J. Phys. Chem. A* **2009**, *113*, 10119−10124.
(58) Fujii, H. *J. Am. Chem. Soc.* **1993**, *115*, 4641−4648.